A new model of the L-H transition in tokamaks

W.Fundamenski[1,2], F.Militello[1], D.Moulton[2], D.C.McDonald[1]

[1] *Culham Centre for Fusion Energy, Abingdon, UK*
[2] *Imperial College of Science, Technology and Medicine, London, UK*

July 14, 2011

Outline of the Presentation

Outline

Motivation I

- Access to the high confinement (H-mode) regime is critical for the commercial viability of fusion energy by magnetic confinement, especially for tokamaks, e.g., ITER. Yet, after more than a quarter of a century since the discovery of the H-mode on the ASDEX tokamak, an adequate model of the L-H (low-to-high confinement) transition is yet to be developed, despite multiple attempts.
- Since auxiliary heating power is expensive, and hence limited, the principle task of any model of the L-H transition is to reproduce and explain the variation of the minimum power for accessing the H-mode, P_{L-H}, with the main engineering quantities.
- This include primarily the observed scaling of P_{L-H} with the toroidal magnetic field, B, the plasma (electron) density, n_e, and the plasma surface area, $S_\perp$, at medium to high density [Martin2008],

$$P_{L-H} \propto B^{0.803\pm0.03} n_e^{0.717\pm0.04} S_\perp^{0.94\pm0.02} \quad (1)$$

Motivation II

- Moreover, the (relatively weak) variation with the cylindrical safety factor, $q_{cyl} = 2\pi\epsilon\kappa aB/(\mu_0 I_p)$ should be reproduced.
- Additional dependencies include inverse aspect ratio, ϵ, ion mass, A, and charge, Z, the poloidal field topology, and Scrape-off Layer (SOL) and divertor geometry, etc. The influence of all these factors on the access power should be captured by any successful model.
- In this letter, we propose a first principles model of the L-H transition, which can explain and correctly predict the functional dependance of P_{L-H} on most of the above factors.
- The model does not address the subsequent edge transport barrier evolution, saturation and relaxation, and is hence only a partial explanation of the H-mode phenomena.

Outline

L-H transition caused by edge plasma dynamics

- As our starting Ansatz, we postulate that the L-H transition is mainly a consequence of edge plasma dynamics, and that it begins in the edge region ($r_\star < r_{LCFS} \equiv a$, where r is the radial co-ordinate and a is the minor radius), in close vicinity of the last closed flux surface (LCFS) and/or the ideal magnetic separatrix, i.e.,

$$a - L_p < r_\star < a, \tag{2}$$

  where $L_p \approx |\nabla_\perp p/p|^{-1}$ is the mean pressure gradient length.
- Hence, the L-H transition should depend on local magnetic field structure and local plasma parameters and their gradients.

L-H transition criterion: $L \rightarrow H \Leftrightarrow Wa > Wa_{L-H}$

Next, we conjecture that the L-H transition occurs when the *Wagner number*, defined below, exceeds some critical value, Wa_{L-H}, which is a constant comparable to unity,

$$\tau_{\parallel}^{A}/\tau_{\perp}^{Q} \equiv Wa > Wa_{L-H} = const \sim 1, \tag{3}$$

In this definition,

$$\tau_{\parallel}^{A} \equiv L_{\parallel}(r_{\star})/V_{A}(r_{\star}), \tag{4}$$

is the Alfvénic time at the radial location, $r_{\star}$, of the L-H transition, and

$$\tau_{\perp}^{Q} \equiv L_{\perp}^{corr}(r_{\star})/V_{\perp}^{Q}(r_{\star}). \tag{5}$$

is the perpendicular energy transport time at $r_{\star}$ over a radial correlation length of a turbulent eddy.

Rationale I

- This is the core hypothesis of the model, since it expresses a *criterion* for the L-H transition.
- It is motivated by stratified magnetohydrodynamics (MHD), where Alfvén waves can stabilize the R-T instability if the Alfvénic time is shorter than the interchange time [Fundamenski2010].
- In tokamak plasmas, which can be described as stratified drift-hydrodynamics (DHD), we would expect the Alfvén waves to play an important role in drift-wave turbulence.
- Indications of this role are present in the literature since the early days of plasma physics and span from Kadomtsev, who described the linear coupling between the drift and Alfvén waves, to the works of Scott Scott and Rogers et al., in which drift-waves induced turbulent transport in the edge is shown to be significantly affected by electromagnetic effects.

Rationale II

- A recurring theme is the strong coupling of these waves as their characteristic times become comparable. When this happens, the electron response is no longer adiabatic and a robust nonlinear drift-wave instability can occur.
- This, in turn, can enhance the inverse energy cascade, leading to velocity shears associated with zonal flows and, as a consequence, to turbulence quenching.
- In other words, a new channel becomes available at the transition, in which the energy of the turbulence can flow and be redirected to harmless (from the confinement point of view) axysimmetric perturbations.

Magnetic field structure near the separatrix

- Our next task is to obtain expressions for $L_{\|}$, $L_{\perp}^{corr}$ and $V_{\perp}^{Q}$ which appear in Eqns 4 and 5.
- To estimate $L_{\|}$ in the vicinity of the separatrix one needs to consider the nature of the magnetic field in the edge region of divertor tokamaks.
- The KAM theorem predicts the separatrix to be a fragile object, i.e., unstable to tiny perturbations. This fragile object, on which ideally $L_{\|} \propto q_{sep} \rightarrow \infty$, breaks up into a thin stochastic layer, in which the magnetic field has a 3-D structure.
- As a result, q_{sep} saturates at some finite value, which scales weaker than linearly with q_{cyl} [Punjabi1994].

Magnetic field structure near the separatrix

Due to the presence of the stochastic layer, we may assume $q_\star$ to scale weaker than linearly with the plasma current, e.g., with a square root dependence,

$$q_\star \approx \alpha_\star q_{cyl}^{1/2}, \qquad L_\parallel^\star \approx \pi q_\star R, \tag{6}$$

where $\alpha_\star > 1$ is a free parameter in the model and $L_\parallel^\star \approx 2\pi q_\star R$ is the parallel length at $r_\star$.

Since the effect of the magnetic perturbation is likely to be much weaker on the open field lines, we assume that the safety factor in the near SOL, $q_\odot$ is linear proportional to q_{cyl},

$$q_\odot \approx \alpha_\odot q_{cyl}, \qquad L_\parallel^\odot \approx \pi q_\odot R. \tag{7}$$

where $\alpha_\odot \approx 1$ is a free parameter and $L_\parallel^\odot$ is the connection length in the near-separatrix SOL.

Eddy size taken as the meso-scale

Motivated by recent JET measurements [Xu2009], we estimate the radial correlation length of a turbulent eddy by the meso-scale,

$$L_{\perp}^{corr} \approx \sqrt{L_p \rho_S}, \tag{8}$$

consisting of a logarithmic average of the mean pressure gradient length, L_p, and the ion gyro-radius evaluated at the cold-ion plasma sound speed, ρ_S,

$$\rho_S = \frac{C_S}{\Omega_i} = \sqrt{\frac{ZT_e}{m_i}}\left(\frac{m_i}{ZeB}\right) \approx (T_e/\zeta])^{1/2}(eB)^{-1} \propto (A/Z)^{1/2} T_e^{1/2} B^{-1}, \tag{9}$$

where $\zeta = \sqrt{Z/Am_p}$ (we assume a two species plasma, so that $n_e = Zn_i$ and $m_i = Am_p$). Hence, Eqn 8 evaluated at $r_\star$ gives $L_{\perp}^{corr}(r_\star) \approx \sqrt{L_p(r_\star)\rho_S(r_\star)}$.

Pressure gradient length assumed to scale as qa

Guided by empirical evidence [Militello2011] we assume that L_p scales linearly with a and the local safety factor, $q_\star$,

$$L_p^\star \equiv L_p(r_\star) \propto a q_\star \propto R \epsilon q_{cyl}^{1/2}, \tag{10}$$

where $\epsilon = a/R$ is the inverse aspect ratio.

Effective radial convective velocity

The radial velocity of electron energy transport, as it appears in Eqn 5, is estimated as

$$V_\perp^Q \equiv Q_\perp/(\tfrac{3}{2}p_e) \equiv P_\perp/[\tfrac{1}{2}S_\perp \times \tfrac{3}{2}p_e], \tag{11}$$

where $P_\perp$ is the power crossing the flux surface, $S_\perp$ is the surface area, and $p_e = n_e T_e$ is the electron pressure.

At $r = r_\star \approx a$, these become

$$P_\perp \approx P_\odot, \quad S_\perp \approx 4\pi^2 R^2 \epsilon\sqrt{\kappa}, \quad p_e = p_e(r_\star), \tag{12}$$

where $P_\odot = P_{heat} - P_{rad}^{core}$ is the power entering the SOL and κ is the plasma elongation.

Temperature and density estimated by the two point model

To approximate the temperature and density at the $L-H$ transition location, $r_\star < a$, we take their near-separatrix SOL values, $r_\odot > a$, i.e., we assume that the radial gradient across the thin stochastic layer is small. This permits us to use the so-called two point model of SOL transport [Stangeby2000], to estimate the electron temperature and density at $r_\odot$ as the the 'upstream' SOL values in the two point model, using

$$T_{eu}^{7/2} \approx T_{et}^{7/2} + \tfrac{7}{4} P_\odot L_\parallel^\odot / (S_\parallel \kappa_{0e}), \tag{13}$$

where T_{eu} and T_{et} are the upstream and target values of the temperatureand $\kappa_{0e} \propto A^0 Z^{-1}$ is a constant in the Spitzer-Harm expression for parallel heat conduction, $\kappa_{\parallel e} = \kappa_{0e} T_e^{5/2}$ [Spitzer1953]. This relation follows directly from a quadrature of the parallel electron heat conduction equation,

$$P_\odot / S_\parallel = Q_{\parallel e} \approx \kappa_{\parallel e} \nabla_\parallel T_e = \kappa_{0e} T_e^{5/2} \nabla_\parallel T_e, \tag{14}$$

between the upstream and target regions.

Temperature and density estimated by the two point model

The target temperature in Eqn 13 may be obtained by invoking two additional assumptions of the 2 point model: (i) pressure conservation,

$$(1 + M_{\|u}^2) n_u T_u \approx (1 + M_{\|t}^2) n_t T_t \quad \Rightarrow \quad n_u T_u \approx 2 n_t T_t,$$

where the right hand size follows on account of the Bohm sheath condition ($M_{\|t} \approx 1$) and near stagnant upstream SOL ($M_{\|u} \ll 1$), and (ii) the target energy flux boundary condition,

$$P_\odot / S_\| = Q_{\|t} = \gamma T_{et} n_{et} C_{St}, \quad \Rightarrow \quad T_{et} \approx \left(P_\odot / S_\| \gamma \zeta n_{et} \right)^{2/3}$$

where $\gamma = \gamma_e + \gamma_i \approx 8$ is the sheath energy transmission coefficient. The parallel energy flow (cross-sectional) area, $S_\|$, may be derived from a divergence form of energy conservation, $\nabla_\| Q_\| \approx \nabla_\perp Q_\perp$,

$$S_\| = S_\perp (L_\perp / L_\|)_\odot \approx 4\pi R \sqrt{\kappa} \lambda_Q \epsilon / q_\odot. \tag{15}$$

where $\lambda_Q = |\nabla_\perp Q_\| / Q_\||^{-1} \approx \int Q_\| dr / Q_{max}$ is the radial power width in the SOL.

Power decay length in the SOL

Finally, the power e-folding length in the near-separatrix SOL, appearing in Eqn 15, is estimated as

$$\lambda_Q \approx V_\perp \tau_{\|Q}, \tag{16}$$

where $V_\perp$ is the effective radial transport velocity and

$$\tau_{\|Q} \approx \tau_{\|T} \approx L_\|^2/\chi_{\|e} \tag{17}$$

is the parallel energy removal time, which is assumed here to be dominated by parallel electron conduction. Combining Eqn 16 and Eqn 17 yields

$$\lambda_Q \propto \pi q_\odot R(Z/A)^{1/2}\nu_\odot \propto R q_{cyl}(Z/A)^{1/2}\nu_\odot, \tag{18}$$

where $\nu_\odot = L_\|^\odot/\lambda_{ei} \propto Z n_{eu} L_\|^\odot/T_{eu}^2$ is plasma collisionality in the upstream SOL near the LCFS. Combing Eqn 7, Eqn 15 and Eqn 16, and noting that $L_\|^\odot$ cancels in the process, the ratio $L_\|^\odot/S_\|$ may be obtained as

$$L_\|^\odot/S_\| \propto (4\pi R\sqrt{\kappa} M_\perp^\odot (Z/A)^{1/2}\nu_\odot \epsilon/q_\odot)^{-1}. \tag{19}$$

where $M_\perp^\odot = V_\perp/C_S$ is the near-SOL perpendicular Mach number.

Outline

Predicted P_{L-H}

The L-H transition criterion, Eqn 3, may now be written explicitly as

$$Wa(r_\star) \equiv \frac{\tau_\parallel^A(r_\star)}{\tau_\perp^Q(r_\star)} = \frac{L_\parallel(r_\star)/V_A(r_\star)}{L_\perp^{corr}(r_\star)/V_\perp^Q(r_\star)} \approx 1. \tag{20}$$

Inserting the estimate of $V_\perp^Q(r_\star)$, Eqn 11, this becomes

$$P_{L-H} \approx \tfrac{3}{2} p_{e\star} S_\perp V_{A\star} L_\perp^{corr\star}/L_\parallel^\star, \tag{21}$$

with all terms evaluated at $r_\star$.

Predicted P_{L-H} scaling in terms of temperature

Recalling that the Alfvén speed is defined as

$$V_{A\star} \equiv \frac{B}{\sqrt{m_i n_{i\star}}} \propto \frac{B}{\sqrt{n_{e\star}}}\sqrt{\frac{Z}{A}}, \tag{22}$$

and using Eqn 8 and Eqn 6 to eliminate $L_{\perp}^{corr}$ and $L_{\|}$, one finds

$$P_{L-H} \propto \frac{3}{2} n_{e\star} T_{e\star} S_{\perp} \frac{B}{\sqrt{n_e}} \sqrt{\frac{Z}{A}} \frac{\sqrt{L_p \rho_S}}{\pi q_\star R}, \tag{23}$$

which, using Eqns 6, 9 and 10 simplifies to

$$P_{L-H} \propto (n_{e\star} B \kappa / q_\star)^{\frac{1}{2}} (R\epsilon)^{\frac{3}{2}} (Z/A)^{\frac{1}{4}} A^{-\frac{1}{4}} T_{e\star}^{\frac{5}{4}} \tag{24}$$

Temperature scaling: two regimes of SOL transport

We can now combine Eqn 13 and Eqn 15 to find an explicit expression for the SOL upstream temperature, and hence for $T_{e\star} \approx T_{e\odot} = T_{eu}$,

$$T_{e\star} \approx T_{e\odot} \approx \left[\left(\frac{P_{L-H}}{S_{\|}} \frac{1}{\gamma \zeta n_{et}} \right)^{\frac{7}{3}} + \frac{7}{4} \frac{P_{L-H} L_{\|}^{\odot}}{\kappa_{0e} S_{\|}} \right]^{\frac{2}{7}} \tag{25}$$

The two terms appearing in Eqn 25 correspond to two distinct regimes of SOL transport:

- the left term dominates in the sheath limited (or low recycling) regime in which $1 < T_{eu}/T_{et} < 2$, and
- the right in the conduction limited (or high recycling) regime, $T_{eu}/T_{et} > 2$.

The transition between these two regimes, defined as the point at which $T_{eu}/T_{et} \approx 2$, occurs at some critical value of the SOL collisionality, typically at $\nu_{\odot} \approx 15$ [Stangeby2000].

Predicted P_{L-H} scaling at high density ($\nu_\odot \gg 15$)

In the *conduction limited* regime, i.e., for $\nu_\odot \gg 15$, when $T_{eu}^{7/2} \gg T_{et}^{7/2}$, Eqn 25 becomes

$$T_{e\star}^{cd} \approx T_{e\odot}^{cd} = T_{eu}^{cd} \approx \left[\frac{7}{4}\frac{P_{L-H}L_{\parallel}^{\odot}}{\kappa_{0e}S_{\parallel}}\right]^{\frac{2}{7}} \tag{26}$$

Inserting Eqn 19 into Eqn 26, we find

$$T_{e\star}^{cd} \propto \left[\frac{P_{L-H}q_\odot Z}{R\epsilon(Z/A)^{1/2}\nu_\odot}\right]^{\frac{2}{7}}. \tag{27}$$

Finally, inserting into Eqn 24, and simplifying we find the desired scaling for P_{L-H},

$$P_{L-H}^{cd} \propto (n_{e\star}B/\sqrt{A}q_\star)^{\frac{7}{9}}(R\epsilon)^{\frac{16}{9}}\kappa^{\frac{1}{2}}q_\odot^{\frac{5}{9}}(Z/A)^{\frac{1}{9}}Z^{\frac{5}{9}}\nu_\odot^{-\frac{5}{9}}. \tag{28}$$

Predicted P_{L-H} scaling at high density ($\nu_\odot \gg 15$)

Since the P_{L-H} size scaling is generally reported in terms of $S_\perp$ rather than R, it is useful to express the minor radius, $R\epsilon = a$, in terms of the surface area, $S_\perp$, Eqn 12, which gives $a = R\epsilon \propto (S_\perp \epsilon)^{1/2}\kappa^{-1/4}$. Inserting this form into Eqn 28, introducing dependence of $q_\star$, Eqn 7, and $q_\odot$, Eqn 6, on the plasma current via q_{cyl}, and noting that $\nu_\star/\nu_\odot \propto q_\star/q_\odot \propto q_{cyl}^{-1/2}$, we find

$$P_{L-H}^{cd} \propto (n_{e\star}B)^{\frac{7}{9}}(S_\perp\epsilon)^{\frac{8}{9}}\kappa^{\frac{1}{18}}g^{cd}(A,Z)h^{cd}(q_{cyl},\nu_\odot). \tag{29}$$

$$g^{cd}(A,Z) = (Z/A)^{\frac{1}{9}}A^{-\frac{7}{18}}Z^{\frac{5}{9}} = A^{-1/2}Z^{2/3}, \tag{30}$$

$$h^{cd}(q_{cyl},\nu_\odot) = q_\star^{-\frac{7}{9}}q_\odot^{\frac{5}{9}}\nu_\odot^{-\frac{5}{9}} \propto q_{cyl}^{\frac{1}{6}}\nu_\odot^{-\frac{5}{9}}. \tag{31}$$

Predicted P_{L-H} scaling at low density ($\nu_\odot \ll 15$)

A similar calculation in the *sheath limited* regime, i.e., for $\nu_\odot \ll 15$, when $T_{eu} \approx T_{et}$, so that Eqn 25 becomes

$$T_{e\star}^{sh} \approx \left(P_{L-H}/S_{\|}\gamma\zeta n_{et}\right)^{\frac{2}{3}}, \tag{32}$$

yields

$$P_{L-H}^{sh} \propto n_{e\star}^{-2} B^3 S_{\perp}^{-\frac{1}{2}} \epsilon^{\frac{9}{2}} \kappa^{\frac{3}{4}} g^{sh}(A,Z) h^{sh}(q_{cyl},\nu_\odot). \tag{33}$$

$$g^{sh}(A,Z) = (A/Z)[A/(Z+1)]^{\frac{5}{2}} A^{-\frac{3}{2}} \approx A^2 Z^{-9/4}, \tag{34}$$

$$h^{sh}(q_{cyl},\nu_\odot) = q_\star^{-3/2} \nu_\odot^{-5}. \tag{35}$$

Outline

Comparison with experiment: scalings

Quantity: $P_{LH} \propto$	Model $(\nu_\odot \ll 15)$	Model $(\nu_\odot \approx 15)$	Model $(\nu_\odot \gg 15)$	Experiment $(\nu_\odot > 15)$
B	3	1.4	0.78	0.82
n_e	-2	0	0.78	0.72
$S_\perp$	-0.5	0.5	0.89	0.94
ϵ	2	1.9	0.89	≈ 1
κ	0.055	0.055	0.055	≈ 0
δ	0	0	0	≈ 0
q_{cyl}	-0.75	-0.3	0.16	≈ 0
$q_\star$	-1.5	-1.4	-0.78	< 0
$q_\odot$	0	0.4	0.55	> 0
A	2	0.2	-0.5	≈ -1
Z	-2.25	-0.15	0.66	0.7 (Z_{eff})

Comparison with experiment: scalings

- The low and high density asymptotic scalings are summarized in the Table (previous slide).
- The latter are in good agreement with the observed P_{L-H} scaling exponents at high density, Eqns 1, also shown in the Table.
- The model also reproduces the observed weak scaling with q_{cyl}, while the predicted scalings with $q_\star$ and $q_\odot$ are qualitatively consistent with the observed dependance of P_{L-H} on limiter vs divertor SOL (much higher in the former), single vs double null configurations (higher in the former) and the divertor leg length (increasing with leg length).
- Finally, the model predictions are also consistent with the observed hysteresis in access power, with $P_{H\to L} < P_{L\to H}$.

Comparison with experiment: data

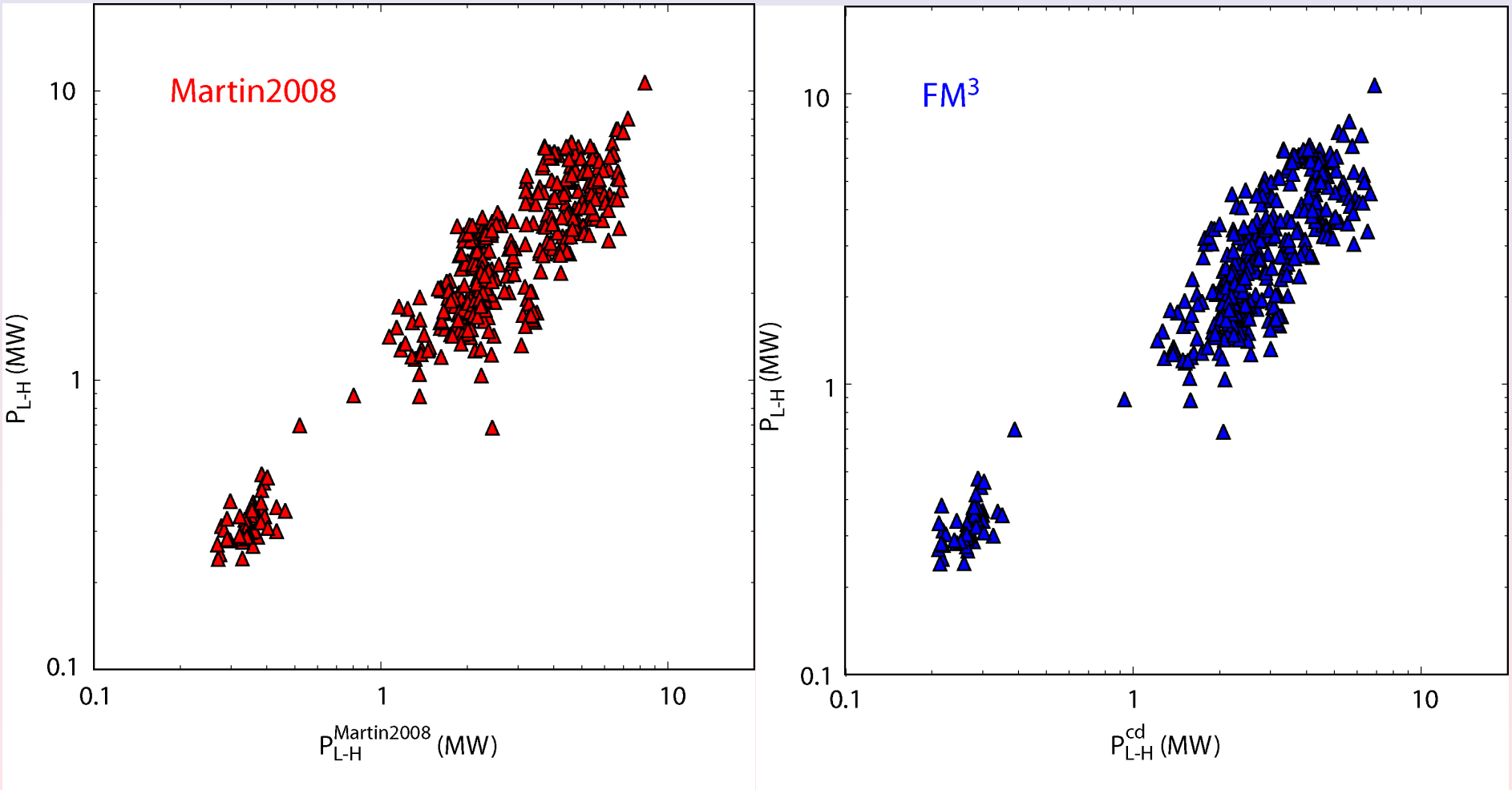

Comparison with experiment: data

- A comparison of the model predictions with experimental measurements of P_{L-H} on several tokamaks, obtained from the ITPA $L-H$ transition database, is shown on the next slide (right frame).
- Also shown is the comparison of the database with the best-fit power law scaling Eqn 1 (left frame), [Martin2008].
- Combined, the two figures reveals a good level of agreement between the model, the empirical scaling and the multi-machine database.

P_{L-H} scaling with plasma density

Since the scaling exponent of P_{L-H} with density is negative at low density and positive at high density, it must be zero at some intermediate density where P_{L-H} has a local minimum. Inserting Eqn 25 into Eqn 24, differentiating with respect to density and simplifying, yields the scaling of the minimum H-mode access power,

$$P_{L-H}^{min} \propto B^{\frac{7}{5}} R \epsilon^{\frac{12}{5}} \kappa^{\frac{1}{2}} g(A,Z) h(q_{cyl}, \nu_{\odot}), \tag{36}$$

$$g(A,Z) = A^{\frac{1}{5}} Z^{\frac{1}{5}} (Z+1)^{-\frac{7}{10}}, \quad h(q_{cyl}, \nu_{\odot}) = q_{\star}^{-\frac{7}{5}} q_{\odot}^{\frac{2}{5}} \nu_{\odot}^{-\frac{9}{5}}.$$

The corresponding minimum density, normalized by the Greenwald density, $n_{GW} \propto I_p/a^2$, is found to scale as

$$f_{GW,L-H}^{min} \propto B^{-\frac{1}{5}} R^0 \epsilon^{\frac{4}{5}} \kappa^{-\frac{1}{2}} g(A,Z) h(q_{cyl}, \nu_{\odot}), \tag{37}$$

$$g(A,Z) = A^{\frac{9}{10}} Z^{-\frac{3}{5}} (Z+1)^{-\frac{9}{10}}, \quad h(q_{cyl}, \nu_{\odot}) = q_{\star}^{-\frac{4}{5}} q_{\odot}^{-\frac{1}{5}} \nu_{\odot}^{-\frac{8}{5}}.$$

This prediction agrees with the observed variation of $f_{GW,L-H}^{min}$, which is roughly independent of R and decreases weakly with B [Martin2008].

P_{L-H} scaling with plasma density for typical JET conditions (3 T, 3 MA, D ions; $L_p \sim 1.5$ cm, $\lambda_q \sim 1$ cm)

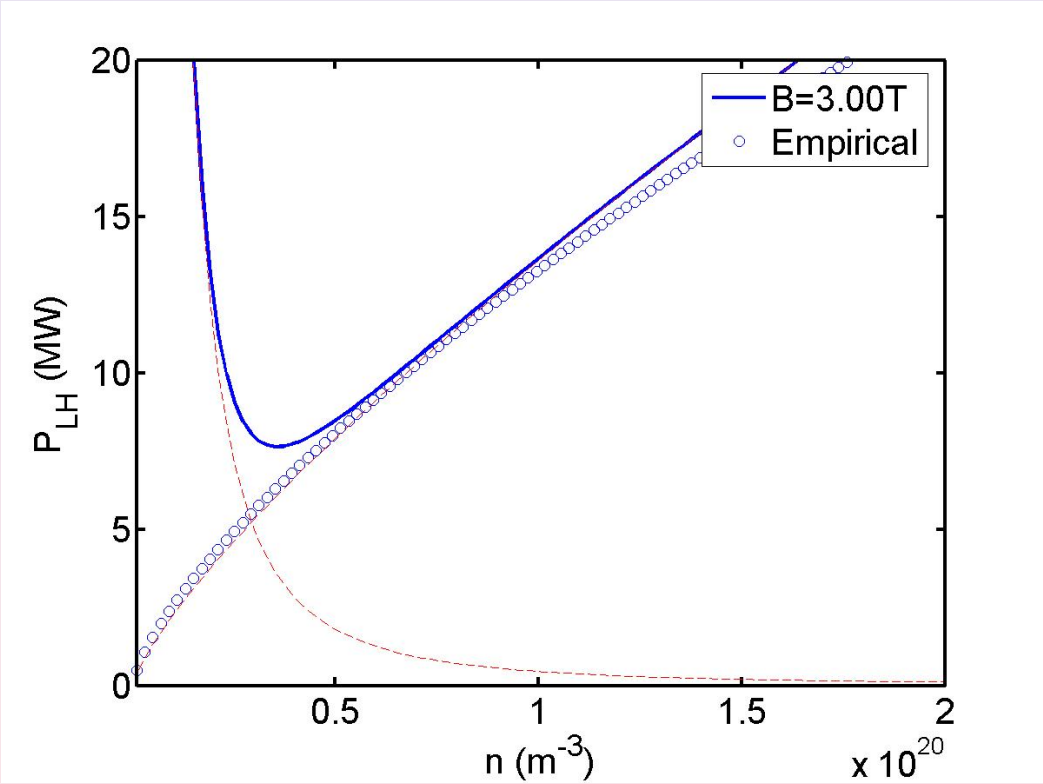

- Note the transition at $f_{GW} \sim 0.3$ from the sheath limited regime at low density to the conduction limited regime at high density.

Outline

Summary

- A first principles model of the L-H transition (but not evolution, saturation or relaxation!) in tokamaks was proposed, based on the criterion that the transition occurs when plasma turbulence and shear Alfvén waves compete in the vicinity of the last closed flux surface.
- The model was used to predict the scaling of the H-mode access power, P_{L-H}, with magnetic and plasma variables.
- The predictions are in good agreement with the experimental scaling of P_{L-H} with plasma size, density, magnetic field and edge safety factor (plasma current).
- They are also qualitatively consistent with the dependance of P_{L-H} on ion mass and charger, limiter vs divertor plasmas, single vs double null configurations, the divertor leg length and H-L vs L-H hysteresis.
- Finally, the model explains the appearance of the minimum in P_{L-H} with plasma density, and correctly predicts the scaling of the density at minimum P_{L-H}.